ELECTRICAL BEHAVIOR OF EPOXY RESIN SUBJECTED TO THERMAL TREATMENT BY TEMPERATURE VARIATION

Article · March 2024

CITATIONS
0

READS
71

13 authors, including:

Costel Paun
University politehnics of bucharest
21 PUBLICATIONS **34** CITATIONS
SEE PROFILE

Doina Elena Gavrila
Polytechnic University of Bucharest
86 PUBLICATIONS **81** CITATIONS
SEE PROFILE

Jana Pintea
Institutul National de Cercetare Dezvoltare pentru Inginerie Electrica ICPE-CA
48 PUBLICATIONS **123** CITATIONS
SEE PROFILE

Victor Stoica
Institutul National de Cercetare Dezvoltare pentru Inginerie Electrica ICPE-CA
31 PUBLICATIONS **116** CITATIONS
SEE PROFILE

ELECTRICAL BEHAVIOR OF EPOXY RESIN SUBJECTED TO THERMAL TREATMENT BY TEMPERATURE VARIATION

Costel PĂUN[1,2], Doina Elena GAVRILĂ[3], Jana PINTEA[4], Veronica MANESCU (PALTANEA)[2,5], Victor STOICA[4], Gheorghe PALTANEA[2], Silviu VULPE[1], Cosmin ROMANIȚAN[1], Vasilica ȚUCUREANU[1], Octavian IONESCU[1], Iuliana MIHALACHE[1], Oana BRÎNCOVEANU[1], Florian PISTRITU[1]

This paper analyzes the behavior of some epoxy resin samples subjected to thermal treatment through temperature variation. After being prepared, the polymeric material was subjected to a temperature variation from +150°C to −20°C during 10 cycles. The effect of thermal cycles on epoxy resin samples was studied with the help of FTIR, SEM, XRD, UV-Vis, electrical, and dielectric measurements. The results show that the thermal treatment to which the samples are subjected produces changes in their structure and morphology and affects the electrical and dielectric properties of the studied epoxy resin.

Keywords: epoxy resin, FTIR, SEM, XRD, UV-Vis, electrical measurements

1. Introduction

In the last decades, polymers have evolved in the electrical insulating materials world production. Insulation materials based on epoxy resin play an increasingly important role due to its special properties. Epoxy resin is a good electrical insulator, has good resistance to corrosion, moisture, and chemicals, and has excellent adhesion to materials and mechanical characteristics. Due to these properties, epoxy resin is mainly used in the electrical, electronic, automotive, aerospace industries [1-3].

Insulating materials made of epoxy resin present a series of shortcomings in long-term operation and special environmental conditions. Defects of epoxy resin-

[1] National Institute for Research and Development in Microtechnologies IMT-Bucharest, Bucharest, Romania, e-mail: pauncostel1986@yahoo.com
[2] Faculty of Electrical Engineering, National University of Science and Technology POLITEHNICA Bucharest, Romania
[3] Faculty of Applied Sciences, National University of Science and Technology POLITEHNICA Bucharest, Romania, e-mail: doina.gavrila@physics.pub.ro
[4] National Institute for Electrical Engineering ICPE-CA, Bucharest, Romania, e-mail: stoica_victor@yahoo.com
[5] Faculty of Material Science and Engineering, National University of Science and Technology POLITEHNICA Bucharest, Romania, e-mail: m1vera2@yahoo.com

based insulating materials may occur due to the following causes: increased brittleness, low anti-crack resistance under low environmental temperature conditions, and rapid change of working temperature from high to very low temperatures.

Electrically insulating materials play a significant role in safely operating electrical devices. Destruction of insulation has devastating consequences for the operation and safety of electrical equipment. Maintaining the optimal parameters of insulating materials as much as possible, even under extreme environmental conditions, is an area of wide interest. So far, research has been done on the thermal degradation of epoxy resin by heat and moisture degradation, and the dielectric and mechanical properties have been studied [4-7].

During the operation of electrical equipment, they are subject to thermal shocks consisting of rapid temperature changes that can lead to the degradation of insulating materials. In order to understand the degradation phenomenon through thermal cycling, in the present study, the samples of epoxy resin material are subjected to accelerated aging in the form of cycles with temperature variation between +150°C and −20°C. Analyses were made using the following techniques to evaluate the degradation of the epoxy resin samples: Fourier transform infrared (FTIR) spectroscopy, X-Ray diffraction (XRD) analysis, Ultraviolet–visible (UV-Vis) spectrophotometry, Scanning Electron Microscopy (SEM), electrical, and dielectric measurements.

2. Materials and Methods

2.1. Epoxy sample preparation method

A two-component kit (Epo-Tek 301, Epoxy Technology Co.) consisting of the epoxy and hardener parts was used to prepare the testing samples. The epoxy resin part (60 grams) was thoroughly mixed with 15 grams of hardener for 5 minutes. The mixture was allowed to stand at pre-reaction for 30 minutes. Next, the mixture was cast in PTFE (Polytetrafluoroethylene) molds, weighing each part on an analytical balance. Using PTFE molds allows easy demolding of cured epoxy specimens. The adhesion between PTFE surface and cured epoxy samples is poor and, in this case, it is not necessary to use a release agent.

The cast epoxy molds were left to stand for 2 hours and cured in a circulation oven at 80°C for 30 minutes. The cured molds were left at room temperature for 24 hours, and after that, the epoxy samples were extracted. All tests were performed after one week to allow the material to reach complete curing with correlated mechanical properties [8-12].

The epoxy resin samples were subjected to accelerated thermal aging in a climate chamber CH 250 TVT (Angelantoni, Italy) with a program for adjusting the

temperature curve and uncontrolled humidity. The temperature in the device is measured with thermocouple sensors.

The epoxy resin samples were tested through thermal cycles following the standard GB/T 2423.22-2002. The upper-temperature level was set to +150℃, the lower temperature level was set to −20℃, and the temperature variation rate was set to 3℃/min. The time of the positive and negative temperature isothermal period was set to 27 minutes. The total period of a thermal cycle lasts 203 minutes. Fig. 1 shows the evolution of the temperature measured in the climatic chamber for a thermal cycle that is repeated according to the imposed studied conditions.

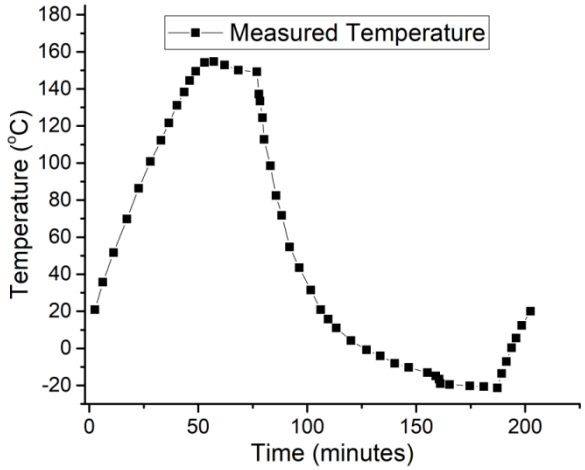

Fig.1. Temperature variation during a single thermal cycle

2.2. Characterization methods

A Cary 5000 UV-Vis-NIR Spectrophotometer (Agilent Technologies, USA) device was used for optical absorption measurements performed at room temperature in the range 350 ÷ 800 nm. The absorbance of each sample was measured after the heat treatment corresponding to the studied cycles.

SEM analysis was performed to evaluate the morphological change related to the effect of thermal cycling using a Nova NanoSEM 630 Field Emission Scanning Electron Microscope (FEI Company, USA). A gold layer of 4 ÷ 5 nm was deposited on the surface of the samples to eliminate the effect of the epoxy resin dielectric properties.

The diffraction spectra were studied using a SmartLab 9kW XRD with rotating anode (Rigaku Corporation, Japan). The measurements were performed on epoxy resin samples with dimensions of 10×10×2 mm^3.

For the structural study, the IR analysis was performed on FTIR spectrometer from Brucker Optics, Tensor 27. The spectra were plotted in the

wavenumber 4000-400 cm^{-1} by averaging 64 scans and with a resolution of 4 cm^{-1}, at room temperature using ATR Platinum holder.

The dielectric constant and the dissipation factor of the epoxy resin samples were measured with an Agilent 4294A impedance analyzer (Agilent Technologies, USA) using a 16451B measuring cell according to the ASTM D150 standard.

The electrical conductivity of the epoxy resin samples was measured using a 4339B high-resistance meter (Agilent Technologies, USA) with a measuring range of up to 4×10^{18} Ωcm employing a 16008B measuring cell. The measurements were performed according to the ASTM 257 standard.

3. Results and discussions

3.1. Color change analysis

The heat treatment changes the color of the epoxy resin samples proportionally to the number of cycles from colorless, yellow, dark yellow, and brown (Fig. 2). This is due to oxidation, the scission of polymer chains and the appearance of carbonyl groups.

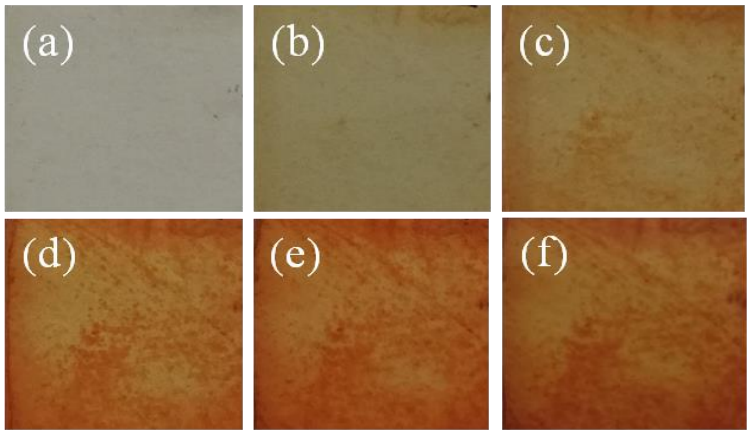

Fig. 2. Digital photo of the epoxy resin samples according to the number of imposed temperature cycles: 0 cycles (neat cured sample) (a), 2 cycles (b), 4 cycles (c), 6 cycles (d), 8 cycles (e), 10 cycles (f).

3.2. UV-Vis results

The absorption spectra corresponding to the 300 ÷ 400 nm wavelength, obtained with UV-Vis spectroscopy are presented in Fig. 3. During the thermal treatment, the molecular weight of the epoxy resin samples increases proportionally with the number of thermal cycles due to the phenomenon of oxidation and cross-linking of the polymer chains. This fact leads to "red-shift" of the maxima to a longer wavelength of the absorption edge of the obtained UV-Vis spectra.

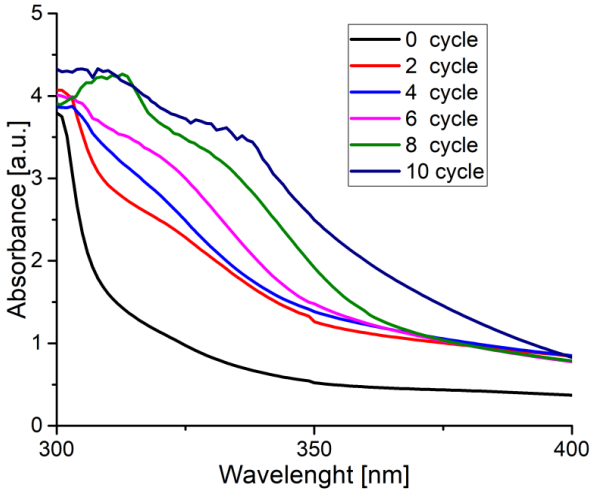

Fig. 3. UV-Vis absorbance curves of epoxy resin samples after each number of imposed thermal cycles.

3.3. FTIR results

The epoxy resin samples were characterized with the FTIR technique. Fig. 4 shows the characterization of the hardened neat epoxy resin. In Table 1, the main peaks of the FTIR spectrum of the epoxy resin were identified [12].

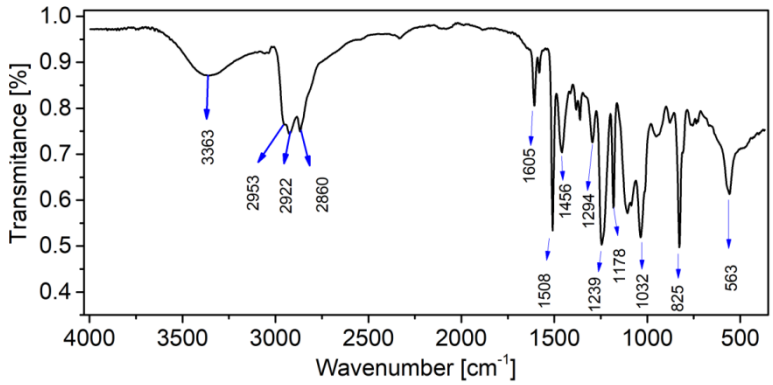

Fig. 4. FTIR spectrum of the neat cured epoxy resin.

Table 1

Possible assignments of the spectral bands for a representative neat epoxy resin sample

Wavenumber (cm^{-1})	Possible assignment
3363	O-H stretching vibration of hydroxyl groups
2953	C-H asymmetrical stretching vibration from $–CH_2$ group.
2922	C-H asymmetrical stretching vibration from $–CH_2$ and CH_3 group
2860	C-H symmetrical stretching vibration from of $–CH_2$ group
1605	C=C bonds in the aromatic skeleton

1508	C=C bonds in the aromatic skeleton
1456	C-H deformation vibration from $–CH_2$ group
1294	C-O deformation vibration from ether
1239	C-O stretching vibration from ether
1178	C-O stretching vibration from ether
1032	C-O stretching vibration from ether
825	C=C deformation vibration.
563	C-H deformation vibration from $–CH_2$ group

During the heat treatment applied to the epoxy resin, polymer chains are split, and free radicals and carbonyl groups (C=O) appear. In the present case, according to Fig. 5a, the appearance of the carbonyl group corresponding to the peak in the FTIR spectrum, at 1654 cm^{-1}, can be observed.

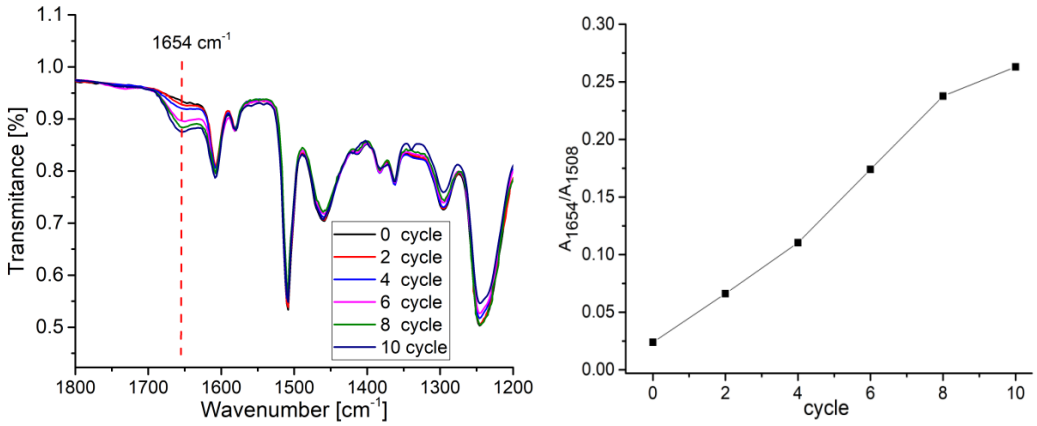

(a) (b)

Fig. 5. FTIR spectra of the epoxy resin in the region 1800 cm^{-1} ÷ 1200 cm^{-1} (a) and evolution of the carbonyl index (CI) values (b) in the case of each number of thermal cycles.

For the calculation of the carbonyl index (CI), the area of the absorption band corresponding to the 1654 cm^{-1} peak was normalized to the area of the absorption band of 1508 cm^{-1}. The obtained results represent an average of 5 measurements. According to Fig. 5b, the carbonyl index (CI) has an upward evolution that can be correlated with the number of applied heat treatments.

3.4. XRD results

In Fig. 6 the resulting diffractogram of the epoxy resin samples corresponding to the thermal treatment show two diffraction bands at 20° and 43°. The width of these bands signifies the amorphous structure of the polymer.

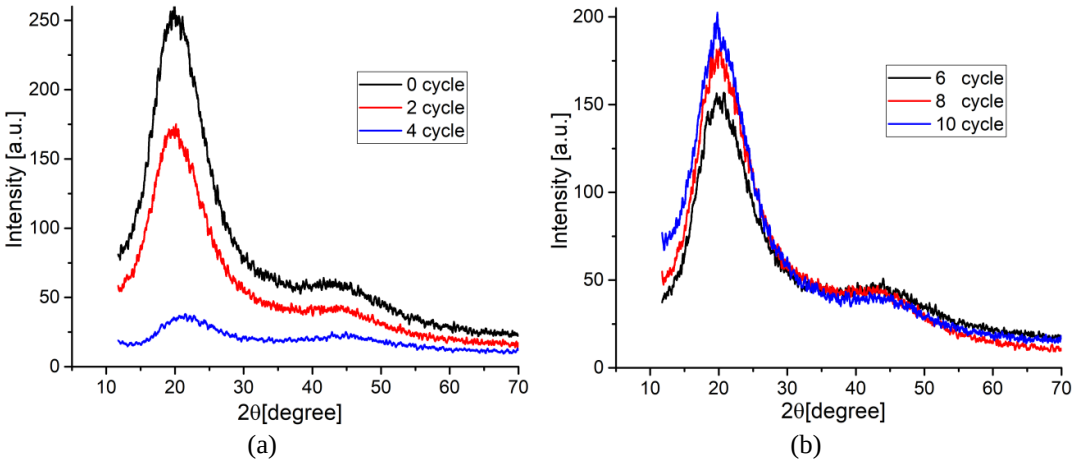

Fig. 6. Diffractogram of epoxy resin corresponding to different number of thermal cycles: 0-4 cycles (a), 6-10 cycles (b).

In the first cycles (Fig. 6a) of the thermal treatment, a process of scission of the polymer chains takes place, resulting in free radicals that combine with oxygen molecules (from diffusion or present in the material) decreasing the degree of crystallinity. In the following cycles (Fig. 6b), the increase in the number of free radicals produced and the depletion of oxygen molecules cause the free radicals to recombine with each other, overcoming the oxidation process. Cross-linking bridges are created between the polymer molecules. Thus, the polymer chains are arranged in a compact structure, which increases the epoxy resin's crystallinity [13, 14].

3.5. SEM results

The non-thermally cycled epoxy resin sample shows no microscopic surface morphology characteristics, only small scratches visible macroscopically due to physical handling. According to Fig.7, the surface of the epoxy resin samples subjected to heat treatment has a different morphology compared to the neat resin samples. The SEM images with a magnification of 600× show after 4 cycles a rough surface of the epoxy resin. After 10 cycles the SEM images show a rougher surface with separated particles and cracks. This fact is due to the scission of the polymer chains during the heat treatment.

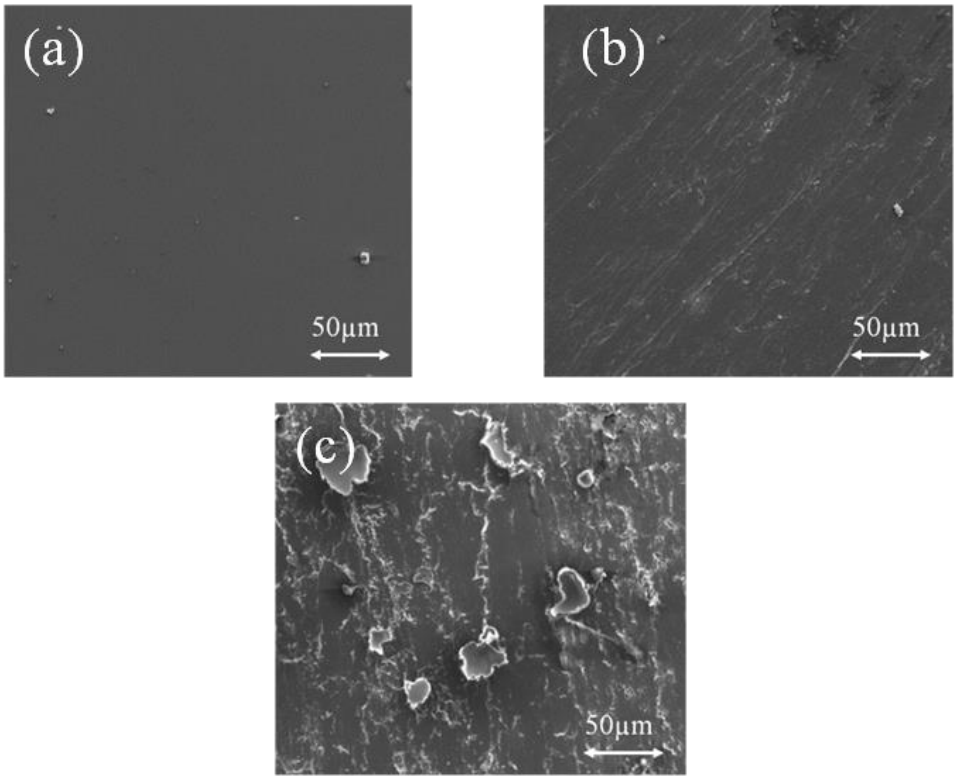

Fig. 7. SEM images of the epoxy resin surface morphology: neat (a), after 4 thermal cycles (b), and after 10 thermal cycles (c).

3.6. Electrical results

Samples of epoxy resin were divided into six groups and subjected to the studied thermal cycles to analyze the behavior of the epoxy resin during the heat treatment. After the completion of the respective processes, the samples were measured, determining the dielectric constant and the dissipation factor on a frequency range from 80 Hz to 100 kHz, as well as the electrical conductivity. The measured data of the dielectric constant and the dissipation factor corresponding to the frequency value of 1 kHz were presented in Table 2.

Table 2

Dielectric constant and dissipation factor values

Cycle	Dielectric constant	Dissipation factor
0	4.7123	0.0065
2	4.3789	0.0099
4	4.4923	0.0136
6	4.8122	0.0124
8	5.1130	0.0139
10	5.7331	0.0151

The electrical conductivity values of the epoxy resin samples are given in Table 3. In Fig. 8, the variation of the dielectric constant spectra against the number of thermal cycles applied to the epoxy resin is presented.

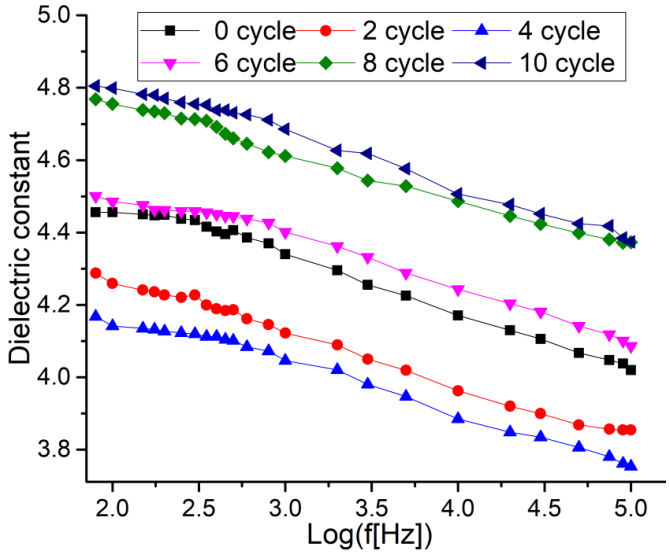

Fig. 8. Dielectric constant versus frequency (logarithmic scale) for the number of thermal cycles.

The dissipation factor spectra vs. the number of thermal cycles are presented in Fig. 9.

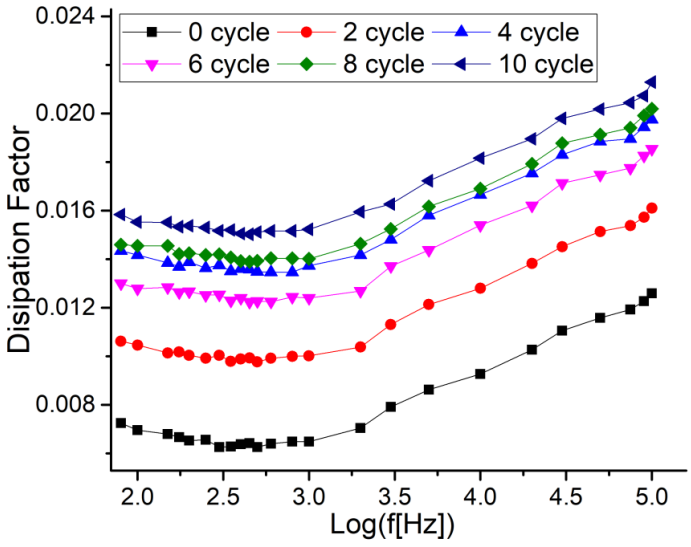

Fig. 9. Dissipation factor versus frequency (logarithmic scale) for the number of thermal cycles.

3.6.1. Dielectric constant results

In the first phase of the thermal treatment, up to 2 cycles, the dielectric constant tends to decrease (Fig. 10). This is due to the post-hardening reaction of the epoxy resin. The post-hardening effect increases the cross-linking density, the molecular level, and the van der Waals force, leading to decreased polarization in the epoxy resin. In the next phase, from 2 to 10 cycles, the dielectric constant has an increasing tendency. This is due to the degradation of the epoxy resin, causing the splitting of the polymer chains and generating an increase in the number of dipoles. Thus, the polarization in the epoxy resin increases [15-22].

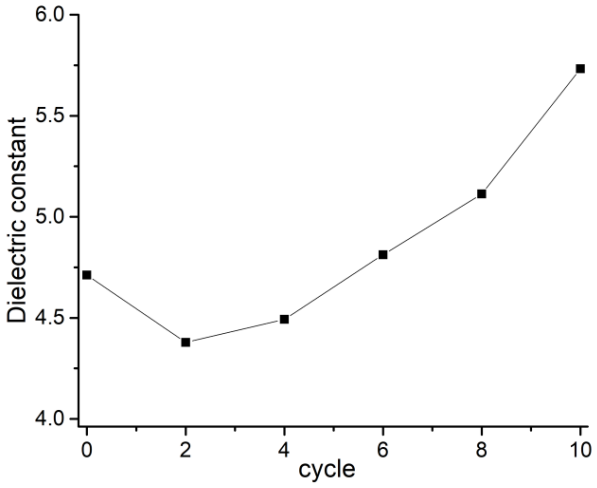

Fig. 10. Variation of the dielectric constant during thermal treatments.

3.6.2. Dissipation factor results

The dissipation factor has an increasing trend up to 4 thermal cycles due to the scission of the polymer chains and implicitly the increase in the concentration of dipoles (Fig. 11). From 4 to 6 cycles, the dissipation factor decreases due to the decrease in polarization in the context of increased crystallinity due to the combination of free radicals. From 6 to 10 cycles, the dissipation factor continued its ascending trend due to the epoxy resin aging, which implies a rapid increase of the polymer chain breaks, resulting in an accentuated increase in polarization.

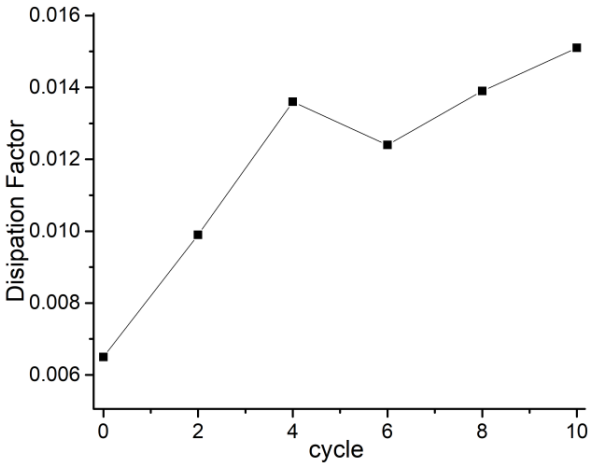

Fig. 11. Variation of the dissipation factor during the thermal treatments.

3.6.3. Conductivity results

Table 3 shows the electrical conductivity values during the thermal treatments.

Table 3

Electrical conductivity values in the case of different number of thermal cycles.

Cycle	Resistivity [Ωm]	Conductivity [S/m]
0	6.6556×10^{9}	1.5023×10^{-10}
2	5.7733×10^{9}	1.7321×10^{-10}
4	5.1461×10^{9}	1.9432×10^{-10}
6	4.2351×10^{9}	2.3612×10^{-10}
8	3.4766×10^{9}	2.8763×10^{-10}
10	3.0011×10^{9}	3.3321×10^{-10}

The electrical conductivity of an insulating material is due to the existence in the material of free electrons, negative or positive ions or the presence of impurities. The presence of the electric field causes these carriers to give rise to an electric current. The magnitude of the current generated in the material is directly proportional to the number of existing carriers [15,23]. In the case studied for the epoxy resin, the majority presence of an ionic conductivity is observed. Polymer chain scission during heat treatment causes the number of free radicals to increase proportionally with thermal cycles. In Fig. 12, it can be observed the increase in the electrical conductivity of the epoxy resin during the thermal cycles.

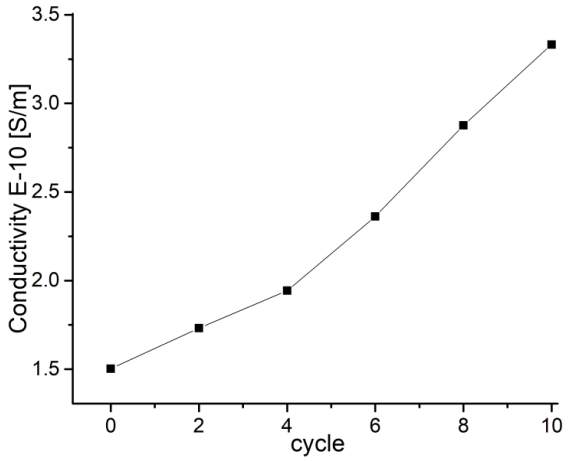

Fig. 12. Variation of the electrical conductivity during the thermal treatment.

4. Conclusions

In the present work, epoxy resin samples subjected to different heat treatment cycles were analyzed. The UV-Vis results show that during the heat treatment, the molecular weight of the epoxy resin increases due to the oxidation and cross-linking process. FTIR analysis shows the oxidation process through the appearance of carbonyl groups. XRD analysis indicates the polymer's crystallinity variation due to oxidation and cross-linking. SEM analysis shows the surface degradation of the thermally cycled samples due to the breaking of the polymer chains. Finally, the electrical analyses show an increase in the dielectric constant, the dissipation factor, and the electrical conductivity during the heat treatment. These results show that in the case of the heat treatment studied, the epoxy resin degrades. These results show that the epoxy resin degrades in the case of the studied heat treatments and, because it constitutes the insulating material, can have devastating consequences for the optimal operation and safety of the respective equipment and devices.

Acknowledgements

The research presented in this paper has been funded by the Ministry of Investments and European Projects through the Human Capital Sectoral Operational Program 2014-2020, Contract no. 62461/03.06.2022, SMIS code 153735 and by a grant of the Ministry of Research, Innovation and Digitization, CNCS-UNEFISCDI, project numbers PN-III-P2-2.1-PED-2021-4158 “Nanocarbon-based resistive sensors for IoT applications–from material synthesis to versatile readout circuitry”.

R E F E R E N C E S

[1]. *F.L. Jin, X. Li, S.J. Park*, Synthesis and application of epoxy resins: a review, Journal of Industrial and Engineering Chemistry, **vol. 29**, 2015, pp. 1-11.

[2]. *T.W. Dakin*, Application of epoxy resins in electrical apparatus, IEEE Transactions on Electrical Insulation, **vol. 4**, 1974, pp. 121-128.

[3]. *C. Paun, C. Obreja, F. Comanescu, V. Tucureanu, O. Tutunaru, C. Romanitan, O. Ionescu, D.E. Gavrila, V. Manescu (Paltanea), V. Stoica, G. Paltanea*, Studies on structural MWCNT/epoxy nanocomposites for EMI shielding applications, IOP Conf. Ser. Mater. Sci. Eng. 1009:012046, https://doi.org/ 10.1088/1757-899X/1009/1/012046, 2021.

[4]. *H. Sepetcioglu, A. Gunoz, M. Kara*, Effect of hydrothermal ageing on the mechanical behaviour of graphene nanoplatelets reinforced basalt fibre epoxy composite pipes, Polym. Polym. Compos., **vol. 29**, 2021, pp. 166-177.

[5]. *R. Zhu, X. Li, C. Wu, L. Du, X. Du, T. Tafsirojjaman*, Effect of hydrothermal environment on mechanical properties and electrical response behavior of continuous Carbon Fiber/Epoxy composite plates. Polymers, **vol. 14**, 2022, 4072.

[6]. *A. Hawa, M.S. Abdul Majid, M. Afendi, H.F.A. Marzuki, N.A.M. Amin, F. Mat, A.G. Gibson*, Burst strength and impact behaviour of hydrothermally aged glass fibre/epoxy composite pipes, Mater. Des., **vol. 89**, 2016, pp. 455-464.

[7]. *Y. Ohki, N. Hirai*, Thermal ageing of soft and hard epoxy resins, High Voltage, **vol. 8**, 2022, pp. 1-9.

[8]. *P.D. McFadden, K. Frederick, L.A. Argüello, Y. Zhang, P. Vandiver, N. Odegaard, D.A. Loy*, UV fluorescent epoxy adhesives from non-covalent and covalent incorporation of coumarin dyes, ACS Appl. Mater. Interfaces, **vol. 9**, 2017, pp. 10061-10068.

[9]. *Q.H. Lin, A.F. Yee, H.J. Sue, J.D. Earls, R.E. Hefner*, Evolution of structure and properties of a liquid crystalline epoxy during curing, Journal of Polymer Science Part B – Polymer Physics, **vol. 35**, no. 14, 1997, pp. 2363-2378.

[10]. *G. Guerriero, R. Alderliesten, T. Dingemans, R. Benedictus*, Thermotropic liquid crystalline polymers as protective coatings for aerospace, Progress in Organic Coatings, **vol. 70**, 2011, pp. 245-251.

[11]. *J.P. Liu, C.C. Wang, G.A. Campbell, J.D. Earls, R.D. Priester*, Effects of liquid crystalline structure formation on the curing kinetics of an epoxy resin, Journal Polymer Science Part A – Polymer Chemistry, **vol. 35**, no. 6, pp. 1105-1124.

[12]. *W.L. Lai, N. Sachdeva, Y.V. Tan, P. Pasbakhsh, H. Saeedipour, K.L. Goh*, Experimental assessment on the mechanical, physical, thermal, and chemical properties of halloysite and carbon nanoparticles reinforced epoxy resins for repair applications, Polym. Adv. Technol., **vol. 34**, 2023, pp. 3260-3275.

[13]. *E.M. Lungulescu, R. Setnescu, S. Ilie, M. Taborelli*, On the use of oxidation induction time as a kinetic parameter for condition monitoring and lifetime evaluation under ionizing radiation environments, in Polymers, **vol. 14**, no. 12, 2022, 2357.

[14]. *T. Zaharescu, M. Râpă, E.M. Lungulescu, N. Butoi*, Filler effect on the degradation of γ-processed PLA/vinyl POSS hybrid, Radiat. Phys. Chem, **vol. 153**, 2018, pp. 188-197.

[15]. *S. Singha, M.J. Thomas*, Dielectric properties of epoxy nanocomposite, IEEE Transactions on Dielectrics and Electrical Insulation, **vol. 15**, 2008, pp. 12-23.

[16]. *S. Singha, M.J. Thomas*, Influence of filler loading on dielectric properties of epoxy-ZnO nanocomposites, IEEE Transactions on Dielectrics and Electrical Insulation, **vol. 16**, no. 2, 2009, pp. 531-542.

[17]. *N.A. Al-Hamdani*, Preparation and electrical properties of epoxy resin reinforced with functionalized carbon nanotubes, IOSR Journal of Applied Physics, **vol. 6**, 2014, pp. 54-56.

[18]. *L.F. Chiriac, P.C. Ganea, D. Manaila Maximean, I. Pasuk, V. Circu*, Synthesis and thermal, emission and dielectric properties of liquid crystalline Eu(III), Sm(III) and Tb(III) complexes based on mesogenic 4-pyridone ligands functionalized with cyanobiphenyl groups, Journal of Molecular Liquids, **vol. 290**, 111184, 2019.

[19]. *D. Manaila Maximean, V. Circu, C.P. Ganea*, Dielectric properties of a bisimidazolium salt with dodecyl sulfate anion doped with carbon nanotubes, Beilstein J. Nanotechnol., **vol. 9**, 2018, pp. 164-174.

[20]. *Z. Wang, Y. Cheng, M. Yang, J. Huang, D. Cao, S. Chen, Q. Xie, W. Lou, H. Wu*, Dielectric properties and thermal conductivity of epoxy composites using core/shell structured Si/SiO_2/polydopamine, Composites Part B: Engineering, **vol. 140**, 2018, pp. 83-90.

[21]. *Y. Wang, Y. Luo, C. Feng*, The influence of temperature and aging on the characteristic parameters of dielectric spectroscopy of epoxy resin impregnated paper insulation, Macromol. Res., **vol. 27**, 2019, pp. 1030-1037.

[22]. *Q. Xie, Y. Cheng, S. Chen, G. Wu, Z. Wang, Z. Jia*, Dielectric and thermal properties of epoxy resins with TiO_2 nanowires, J. Mater. Sci.: Mater. Electron., **vol. 28**, 2017, pp. 17871-17880.

[23]. *A. Boudefel, P. Gonon,* Dielectric response of an epoxy resin when exposed to high temperatures, J. Mater. Sci.: Mater. Electron., **vol.17**, 2006, pp. 205-210.